

## Test of the principle of equivalence by a null gravitational red-shift experiment

John P. Turneaure

*Department of Physics, Stanford University, Stanford, California 94305*

Clifford M. Will

*Department of Physics, Stanford University, Stanford, California 94305  
and McDonnell Center for the Space Sciences, Department of Physics, Washington University,  
St. Louis, Missouri 63130\**

Brian F. Farrell, Edward M. Mattison, and Robert F. C. Vessot

*Center for Astrophysics, Smithsonian Astrophysical Observatory, Cambridge, Massachusetts 02138*

(Received 29 November 1982)

A test of the Einstein equivalence principle (EEP) was performed by carrying out a "null" gravitational red-shift experiment. The experiment compared the rates of a pair of hydrogen maser clocks with those of a set of three superconducting-cavity stabilized oscillator clocks as a function of the solar gravitational potential. If EEP were not valid, the relative rates could vary with potential. During the experiment, the solar potential in the laboratory varied approximately linearly at 3 parts in  $10^{12}$  per day because of the Earth's orbital motion, and diurnally with an amplitude of 3 parts in  $10^{13}$  because of the Earth's rotation. An upper limit on the relative frequency variation of 1.7 parts in  $10^2$  of the external potential was set. The accuracy was limited by the frequency stability of the clocks and by unmodeled environmental effects. The result is consistent with the EEP at the two percent level. The experiment can also be viewed as setting a limit on a possible spatial variation of the fine-structure constant.

### I. INTRODUCTION

One of the key tests of Einstein's principle of equivalence is the gravitational red-shift experiment.<sup>1</sup> Since 1960, when precision red-shift measurements first became feasible, several tests of the principle have been performed, including measurements of the shifts of solar spectra lines, the Pound-Rebka-Snider experiments using  $^{57}\text{Fe}$  nuclear gamma-ray transitions, and comparisons of aircraft-, rocket-, and satellite-borne atomic clocks with ground clocks.<sup>2</sup>

A common feature of these experiments is that they measure the difference in rate between two identical frequency standards located at different points in an external gravitational field. The frequencies are compared either by connecting the two clocks by electromagnetic signals, or by transporting the clocks around closed paths. Every experiment performed to date has confirmed the equivalence principle, the most accurate being the rocket-borne Gravity-Probe *A* red-shift experiment, which verified the predicted frequency shift between a hydrogen maser on Earth and one in a Scout *D* rocket at a

peak altitude of 10 000 km to a precision of 70 parts per million.<sup>3</sup>

A close examination of the content of the principle of equivalence reveals that a valid test would also be provided by a "null gravitational red-shift experiment" in which the rates of two nonidentical clocks at the same location are compared as they move together in a gravitational field. To see this it is useful to state Einstein's equivalence principle (EEP) in its purest form<sup>4,5</sup>: (1) The trajectories of neutral freely falling test bodies are independent of their structure and composition; (2) in local, freely falling frames, the outcome of any nongravitational test experiment is independent of the velocity of the frame; and (3) in local, freely falling frames the outcome of any nongravitational test experiment is independent of where and when in the universe it is performed. (For detailed discussion and definitions see Ref. 4.)

The first part of EEP is called the weak equivalence principle (WEP) and has been verified to high accuracy by Eötvös-type experiments.<sup>2</sup> The second part is known as local Lorentz invariance (LLI) and has been tested by the Hughes-Drever ex-

periment, among others.<sup>5,6</sup> The third part is called local position invariance (LPI), and is the foundation for discussion of red-shift experiments.

A consequence of the validity of EEP is the validity of the postulates of metric theories of gravity: (i) spacetime is endowed with a metric  $g$ ; (ii) test bodies move on geodesics of  $g$ ; and (iii) in local freely falling frames, the nongravitational laws of physics take their special-relativistic forms. An important feature of these postulates is "universality": all the nongravitational interactions, electric, magnetic, weak, and strong, must couple to gravitation in a universal way, as embodied in the "comma goes to semicolon rule." Under this rule the equations of the nongravitational interactions are expressed in Lorentz-invariant form in the local freely falling frame and then are taken over into any frame by replacing the Minkowski metric by the metric  $g$  and ordinary derivatives by covariant derivatives. (See Ref. 7 for further discussion.)

Let us now consider the consequences of EEP for experiments. If EEP is valid, then it is straightforward to show<sup>7</sup> that comparing the rates of two identical clocks at different locations in spacetime involves simply comparing the motions of certain local freely falling frames that momentarily comove with the clocks. Since the clock rates measured in those momentarily comoving frames must be independent of the velocities (LLI) and locations (LPI) of the frames, and since the motion of the frames is universal (WEP), the result is a gravitational "red-shift" that is universal, independent of the nature of the clocks being studied, and that, for weak gravitational fields, is given by

$$Z \equiv \Delta f/f = \Delta U/c^2, \quad (1)$$

where  $f$  is the nominal clock frequency,  $U$  is the Newtonian gravitational potential, and  $c$  is the speed of light.

If, on the other hand, LPI were violated, how would that violation manifest itself? One way might be for clock rates measured in local freely falling frames to depend on location. However, if every type of clock varied in the same manner, there would be no observable violation of LPI, since clock rates are always defined relative to a standard clock. Thus a violation of LPI in clock rates is observable only if at least one kind of clock depends differently on location than the others. Assuming that this violation of LPI is due to nonuniversal coupling to an external gravitational field, then for weak-field situations one would expect the locally measured frequency  $f_A$  of a clock of type  $A$  to vary relative to that of a chosen standard clock (of a different type) at the same location according to

$$f_A = (f_A)_0 [1 - \alpha_A U/c^2 + O((U/c^2)^2)], \quad (2)$$

where  $(f_A)_0$  is the frequency of  $A$  relative to the standard at some fiducial spacetime location from which  $U$  is measured, and  $\alpha_A$  is a dimensionless parameter that measures the extent of LPI violation for clock  $A$ . If LPI is valid,  $\alpha_A = 0$  for any clock type. For a comparison of two clocks of type  $A$  and  $B$ , the relative frequencies would vary, to first order in  $U/c^2$ , according to

$$f_A/f_B = (f_A/f_B)_0 [1 - (\alpha_A - \alpha_B)U/c^2]. \quad (3)$$

Such a comparison—a "null" gravitational red-shift experiment—is therefore a powerful test of LPI and of the equivalence principle.

It is useful to note that, under these circumstances, the usual gravitational red-shift for two identical clocks of type  $A$  would be given by<sup>5</sup>

$$Z = (1 + \alpha_A) \Delta U/c^2. \quad (4)$$

We have performed such a null gravitational red-shift experiment by comparing the frequencies of two hydrogen masers with those of three superconducting-cavity stabilized oscillators (SCSO's) as a function of the solar gravitational potential. The experiment was performed at Stanford University between April 1 and 11, 1978. During this period the solar gravitational potential at the laboratory varied sinusoidally in time with a 24-h period because of the rotation of the Earth and the consequent motion of the laboratory, and also varied approximately linearly with time due to the Earth's eccentric orbital motion. (During the experiment the Earth was approximately 90 degrees from perihelion.) The variation in the solar gravitational potential at the laboratory is given by

$$u \equiv U/c^2 = -3.2 \times 10^{-13} \cos[2\pi(t - t_0)] \\ + 2.8 \times 10^{-12}(t - t_0), \quad (5)$$

where  $u$  is the dimensionless reduced solar gravitational potential,  $t$  is time measured in solar days, and  $t_0 = \text{April } 4.5$ . Making use of the great frequency stabilities of both kinds of clocks (parts in  $10^{14}$  for averaging intervals of roughly 100 seconds) we examined the difference frequencies between the six pairs of unlike clocks for variations having the above signature. In terms of the LPI-violation parameter  $\alpha_{ms} \equiv \alpha_m - \alpha_s$  for hydrogen masers and SCSO's, we obtained the upper limit

$$|\alpha_{ms}| \leq 1.7 \times 10^{-2}. \quad (6)$$

The result is consistent with LPI and the Einstein equivalence principle at the two-percent level.

It might be argued that, because the frequencies

of both hydrogen maser clocks and SCSO clocks depend primarily on electromagnetic interactions, one would not expect them to vary differently. However, a simple example shows that this need not be the case, and provides an alternative interpretation of the experiment.

Suppose that a violation of LPI manifested itself only in a location dependence of the locally measured electromagnetic fine-structure constant  $\alpha$ , so that it depended upon the external gravitational potential. Suppose further that other constants (speed of light, particle masses, strong and weak interaction constants, etc.) were unaffected. Now the nominal frequency of a hydrogen maser is determined by the hyperfine transition in hydrogen, while the frequency of an SCSO is determined by the size of its microwave cavity, and hence by the interatomic spacing in the cavity material. We show in Appendix A that the ratio of the maser and SCSO frequencies is then a function of the atomic fine-structure constant:

$$f_m/f_s \sim [\alpha(U)]^3. \quad (7)$$

From this viewpoint one can conclude that the experiment sets a limit on the spatial variation of the logarithm of the fine-structure constant of 0.007 of the variation of the local gravitational potential. (Some authors have set tighter, though less direct, limits on such a variation by combining the results of Eötvös experiments with an assumption of energy conservation.<sup>8</sup>) Clock intercomparisons of this kind have previously been performed in attempts to search for a time variation in the fine-structure constant, with the result<sup>9</sup>

$$|(1/\alpha)d\alpha/dt| < 4 \times 10^{-12} \text{ yr}^{-1}. \quad (8)$$

From the point of view of local position invariance, we see that these two kinds of measurements are complementary tests of LPI.

In Sec. II below we describe the apparatus and the experimental method, and in Sec. III give the results of the data analysis and discuss possible sources of systematic effects. Section IV discusses the results. Appendix A derives Eq. (7) while Appendix B describes a specific mathematical model for a violation of EEP in electrodynamics, called the  $TH\epsilon\mu$  formalism, and derives explicitly the effects of LPI violation on hydrogen maser and SCSO clocks.

## II. OSCILLATOR CHARACTERISTICS AND EXPERIMENTAL METHOD

The high-stability oscillators used in this experiment were two hydrogen masers built at the Smithsonian Astrophysical Observatory and three

superconducting-cavity stabilized oscillators built at Stanford University. The following discussion of their characteristics is given to help in understanding some of the spurious systematic effects in the data.

The output frequency of the hydrogen maser is based upon the hyperfine splitting of ground-state atomic hydrogen.<sup>10</sup> Hydrogen atoms in the upper hyperfine level ( $F=1$ ,  $m_F=0$ ) enter a Teflon-lined quartz sphere located in an evacuated microwave cavity resonant at the hyperfine transition frequency (1.42 GHz) and are stimulated to radiate to the lower hyperfine level ( $F=0$ ,  $m_F=0$ ) by the microwave field in the cavity. The maser's output frequency is shifted from the unperturbed hyperfine frequency by the atoms's interactions with the Teflon wall surface, with an imposed axial magnetic field, and with each other. The output frequency is also affected by variations in the cavity resonance frequency that can be caused by changes in ambient temperature, barometric pressure, mechanical stress, and other sources.

The SCSO (Ref. 11) consists of an electronic self-oscillator whose frequency-determining element is a high- $Q$  superconducting cavity maintained at the temperature of liquid helium. The cavity's dimensions, and thus its resonance frequency (approximately 8 GHz), can be affected by changes in temperature and in mechanical stress, including stress changes due to variations in the strength of local gravity and in the cavity's angle of tilt relative to the vertical.

The experiment was performed at Stanford University, Palo Alto, California. The three SCSO's were housed in a liquid-helium Dewar in a temperature-controlled, isolated room. The Dewar was equipped with a servo-controlled leveling device to reduce the effect of floor tilt and of change in direction of the local gravitational acceleration on the frequencies of the SCSO's. Two model VLG-10 masers were placed in an adjacent laboratory. Because the temperature of the laboratory was strongly affected by outside weather conditions, a window air conditioner with an on/off control was installed. To moderate the temperature variations caused by the cycling of the air conditioner, the masers were placed in enclosures with temperature-controlled exhaust fans. The frequencies of the oscillators were compared in a multiply-and-mix system that used one of the SCSO's as a reference oscillator. (The SCSO's are referred to as  $S1$ ,  $S2$ , and  $S3$ , and the masers as  $M5$  and  $M6$ . Subscripts indicating frequency differences use numerals only: 1,2,3 for SCSO's and 5,6 for masers.) A 5-MHz voltage-controlled crystal oscillator (VCXO) was phase locked to the output of  $S1$ , and its multiplied output

was mixed with the signals from the four other oscillators to produce beat signals of 1 to 5 Hz. The beat periods were averaged by counters and the average beat period was recorded with the time (epoch) at the end of each measurement.

Thirteen experimental parameters were measured and recorded at 40-min intervals. These included maser temperatures, helium vapor pressure in the SCSO Dewar, Dewar angle of tilt, and other conditions. Local barometric pressure and the variation of the local gravitational acceleration during the period of the experiment were also obtained.

### III. DATA ANALYSIS

#### A. Data preparation

The primary data were four series of averaged beat periods between  $S1$  (arbitrarily chosen as the reference oscillator) and  $S2$ ,  $S3$ ,  $M5$ , and  $M6$ , measured asynchronously at intervals of approximately 250 seconds. These four data sets were transformed into fractional frequency variations  $f_{12}$ ,  $f_{13}$ ,  $f_{15}$ , and  $f_{16}$  (all frequency differences are expressed as fractions of the nominal oscillator frequencies) and spurious points were removed. SCSO  $S1$  was bistable in operation, occasionally switching spontaneously for short times to a higher frequency. The magnitude of this frequency shift is

$$\Delta f/f = 3.5 \times 10^{-14}.$$

All data points lying more than two standard deviations from the local average frequency, including these shifted points, were replaced by values interpolated from adjacent points, the total number of such points representing approximately five percent of the original data. The frequencies were then averaged over synchronous 20-min intervals using a 40-min Hanning filter. The four resulting time series were suitably added together to yield the ten frequency-difference functions that are possible with five oscillators. Representative series are shown in Fig. 1.

The experimental parameter data were interpolated to produce time series in temporal registration with the frequency data. To approximate the response of maser frequency to ambient temperature change, the maser-frame temperatures were smoothed with an exponential filter having a 0.5-day time constant. Of the 13 series of ambient-condition data only three, the vapor pressure of the helium gas in the SCSO Dewar and the temperatures of each of the maser cabinets, had variations that resembled those of the frequency differences. During the first two days of the experiment the helium vapor pressure fell rapidly, with the SCSO frequencies, partic-

ularly that of  $S2$ , showing corresponding rapid shifts. During the eleventh day of the experiment the liquid-helium level fell below a critical level, causing a change of helium pressure and an abrupt change in the SCSO frequencies. To eliminate data that were obviously strongly affected by the vapor pressure we disregarded the data from the beginning and end of the experiment, keeping 8 days of data between days 2.8 and 10.8. (Time is measured in solar days beginning at one minute after midnight on the morning of April 1.)

As shown in Eq. (5), the solar potential  $u$  consists primarily of two terms: a diurnal variation with daily peak-to-peak change of approximately  $6 \times 10^{-13}$ , and a linear variation of approximately  $3 \times 10^{-12}$  per day. Because these terms have different signatures and are masked by separate systematic effects, we used two different regression techniques to search for the presence of the solar potential in the frequency data. Linear regression of  $u$  on the frequency differences, which is sensitive mainly to the linearly varying component of  $u$ , is examined in Sec. III B. A search for the diurnal component is discussed in Sec. III C.

#### B. Linearly varying component of solar gravitational potential

Because the major component of the solar potential is a linear time variation,  $u$  is expected to correlate primarily with linear frequency drifts of the oscillators. Such drifts can also be caused by systematic ambient effects acting on the oscillators or by unidentified internal "aging" drifts. The effects of the helium vapor pressure and of the maser frame temperatures were removed by performing a multi-

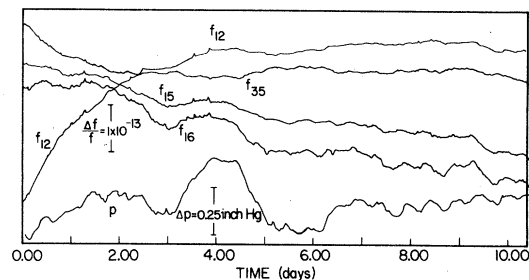


FIG. 1. Selected frequency differences as functions of time. Subscripts 1, 2, and 3 refer to the SCSO clocks, while subscripts 5 and 6 refer to hydrogen-maser clocks. Absolute values of the frequency differences are arbitrary; the vertical scale measures their variation with time. Curve labeled  $p$  shows variations in the ambient barometric pressure. Time is measured in solar days from 12:01 a.m. April 1, 1978.

TABLE I. Regression coefficients of  $u$  on frequency differences  $f_{ij}$ .

Oscillator pair	Regression coefficient $b_{ij}$	Standard error of $b_{ij}$
5-1	$1.45 \times 10^{-2}$	$3.4 \times 10^{-4}$
5-2	$1.25 \times 10^{-2}$	$2.4 \times 10^{-4}$
5-3	$0.57 \times 10^{-2}$	$3.1 \times 10^{-4}$
6-1	$1.50 \times 10^{-2}$	$7.3 \times 10^{-4}$
6-2	$1.39 \times 10^{-2}$	$5.9 \times 10^{-4}$
6-3	$0.67 \times 10^{-2}$	$4.5 \times 10^{-4}$
6-5	$0.30 \times 10^{-2}$	$1.7 \times 10^{-4}$
2-1	$0.36 \times 10^{-2}$	$2.6 \times 10^{-4}$
3-2	$0.58 \times 10^{-2}$	$3.2 \times 10^{-4}$
3-1	$0.93 \times 10^{-2}$	$3.6 \times 10^{-4}$

ple function linear regression on each frequency-difference time series. The independent functions used in the regression were the reduced solar gravitational potential  $u$  and the ambient effects appropriate to the particular frequency difference; for example,  $f_{15}$  was regressed with the helium vapor pressure,  $M5$ 's frame temperature, and  $u$ . Of the ten frequency functions, six (written  $f_{kn}$ ) are frequency differences between dissimilar oscillators (maser-SCSO), and four (written  $f_{rt}$ ) are differences between similar oscillators (maser-maser and SCSO-SCSO). The regression coefficient  $b_{kn}$  of  $u$  on each of the  $f_{kn}$  is proportional to any component of  $f_{kn}$  that varies with the gravitational potential  $u$ , and thus gives a value for  $\alpha_{ms}$ . (Similar oscillators can have no mutual frequency difference induced by  $u$ , so the regression coefficients of  $u$  on the  $f_{rt}$  measure the presence of unidentified systematic effects, or of ambient effects containing linear or diurnal components that were not completely removed by the regression.) The regression coefficients are given in Table I.

The standard errors of the regression coefficients, which are the errors due to scatter of the data about the regression lines, are at most seven percent of the values of the coefficients, while the variations among the coefficients are on the order of magnitude of the coefficients; hence, the errors in determining the individual coefficients (the standard errors) do not significantly affect the variations among coefficients and will be ignored.

Table I shows that the regression coefficients, and thus the relative drift rates, for masers versus SCSO's are all positive (that is, both masers increase in frequency faster than any of the SCSO's), and that the drift rates between dissimilar oscillators are for the most part greater than those between pairs of similar oscillators, indicating that the two groups of

the oscillators are changing frequency at significantly different rates.

The measurements of frequency differences between dissimilar oscillators constitute a group of experiments, each experimental leading to a value for  $\alpha_{ms}$ , from which we wish to determine the mean value  $\alpha_{ms}$  and its confidence interval. We cannot, however, use the six regression coefficients  $b_{kn}$  between dissimilar oscillators to estimate  $\alpha_{ms}$ , because these measurements are not independent. Since the frequency data are related by linear superposition, only four of the six coefficients for dissimilar oscillators are statistically independent. For example, the frequency differences  $f_{51}$ ,  $f_{52}$ ,  $f_{61}$ , and  $f_{63}$  produce the differences  $f_{53}$  and  $f_{62}$ ; therefore the regression coefficients  $b_{53}$  and  $b_{62}$  are related to  $b_{51}$ ,  $b_{52}$ ,  $b_{61}$ , and  $b_{63}$  by linear superposition. Of the fifteen sets of four coefficients that can be chosen from the six  $b_{kn}$ , three sets are not complete in that they do not generate the remaining two coefficients; these sets are  $(b_{51}, b_{52}, b_{61}, b_{62})$  and  $(b_{52}, b_{53}, b_{52}, b_{63})$ , and  $(b_{53}, b_{51}, b_{63}, b_{61})$ . The remaining 12 sets of coefficients represent different ways of measuring  $\alpha_{ms}$ , that is, they can be regarded as 12 possible sets of 4 independent experiments. As we have seen, however, the sets are not independent of one another, and we must choose the average regression coefficient  $\bar{b}$  of one set to estimate  $\alpha_{ms}$ .

Of the 12 values of  $\bar{b}$ , the largest is  $1.25 \times 10^{-2}$  and the smallest is  $0.99 \times 10^{-2}$ . The span between these is less than the typical standard error of approximately  $0.4 \times 10^{-2}$ , indicating that our conclusion is not sensitive to the choice of data set. The largest standard deviation for  $\bar{b}$  for any set is  $0.48 \times 10^{-2}$ .

To estimate an upper bound for  $\alpha_{ms}$  we use the largest value for  $\bar{b}$  and the largest standard deviation. The  $t$  distribution with three degrees of freedom gives the upper bound of the 95-percent confidence interval for  $\alpha_{ms}$  (linear) as

$$|\alpha_{ms} \text{ (linear)}| \leq 2.0 \times 10^{-2}. \quad (9)$$

We label this quantity "linear" because its value is sensitive primarily to the linear component of  $u$ .

### C. Diurnal component of solar gravitational potential

Because the diurnal component of  $u$  is an order of magnitude smaller than the linearly varying component, the regression calculation described in Sec. IIIB is relatively insensitive to the diurnal component. This was verified by a regression calculation on the frequency data in which the diurnal term was treated separately from the linear term; this yielded no significant diurnal component at the 95-percent confidence level. In order to search for a

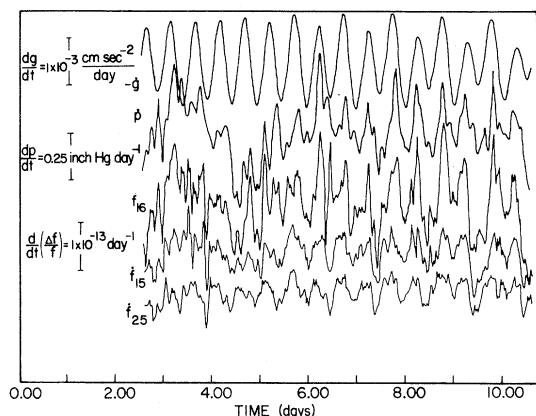


FIG. 2. Time derivatives of frequency-difference series, ambient parametric pressure, and local gravitational acceleration.

gravitational effect without being obscured by long-term drifts we used several time-series analysis techniques to examine the data for the presence of a diurnal variation in phase with the solar gravitational potential. This approach also enabled us to take into account two systematic effects, atmospheric pressure and gravity tides, that have diurnal and semidiurnal variations.

The frequency difference series show substantial long-period fluctuations with durations from fractions of days to several days. This nonstationary behavior is characteristic of noise produced by a first-order autoregressive process, that is, one with the ability to integrate past effects. The noise has a distinctly low-frequency character. In order to detect shorter-period (diurnal) variations, we removed the low-frequency noise by transforming the frequency functions with the time derivative, which is the inverse of the autoregressive process. Figure 2 shows the time derivatives of typical frequency series; short-term variations with periods of approximately one-half day are clearly visible. (We henceforth refer to these time derivatives of the frequency series as derivatives series or frequency derivatives.) The autocorrelation functions of the frequency derivatives, as well as Fourier transforms of the frequency data, show that the dominant periodicity of several of the frequency series is approximately 0.51 days. We confirmed these period estimates with greater precision by means of nonlinear least-squares regression in which a trigonometric function is fitted to the data by adjusting the amplitude, period, and phase of the function. The period of the semidiurnal perturbation determined by this method is  $0.507 \pm 0.002$  solar days. This is significantly longer than half a solar day and suggests the effect of the lunar gravitational tide.

Possible mechanisms of lunar perturbations are changes in the local gravitational acceleration  $g$  (the effect that causes the ocean tides) and variations in the atmospheric pressure  $p$ , which is affected by the variation in  $g$ . To verify the source of the perturbation we cross correlated the derivatives of the frequency differences with the time derivative  $\dot{g}$  of the calculated value of local  $g$  and with the derivative  $\dot{p}$  of the barometric pressure measured at Palo Alto during the experiment. Both correlations were significant, the closer being between the frequency derivative and the barometric pressure derivative. The correlations of the derivative series in Fig. 2 with  $\dot{p}$  and  $\dot{g}$  are striking.

To search for the presence of a solar diurnal component in the frequency derivatives we regressed  $\dot{u}$ ,  $\dot{p}$ ,  $\dot{g}$ , and the appropriate experimental parameters (helium vapor pressure and maser temperature derivatives) on the  $f_{ij}$ . The regression coefficients  $a_{ij}$  for  $\dot{u}$  are given in Table II. Because the functions in the regression were adjusted to zero mean, the  $a_{ij}$  can contain contributions only from the diurnal component of  $\dot{u}$ .

For oscillator pairs involving maser  $M6$  the regression coefficients, which measure the sensitivity of the oscillators' frequencies to changes in barometric pressure, are substantially larger than for most other oscillator pairs. The source of this difference, and its possible effect on the results of the experiment, are discussed in Sec. IV B.

As discussed in Sec. III B, only quartets of the six coefficients  $a_{kn}$  between dissimilar oscillators can be regarded as independent estimates of  $\alpha_{ms}$ . The largest mean regression coefficient  $\bar{a}$  for any such set is  $1.00 \times 10^{-2}$  and the largest standard deviation for  $\bar{a}$  is  $0.41 \times 10^{-2}$ . From these values the greatest upper bound of the 95-percent confidence interval for  $\alpha_{ms}$  (diurnal) is

TABLE II. Regression coefficients of  $\dot{u}$  on frequency derivatives  $f_{ij}$ .

Oscillator pair	Regression coefficient $a_{ij}$	Standard error of $a_{ij}$
5-1	$-0.51 \times 10^{-2}$	$0.17 \times 10^{-2}$
5-2	$-0.16 \times 10^{-2}$	$0.12 \times 10^{-2}$
5-3	$-0.34 \times 10^{-2}$	$0.12 \times 10^{-2}$
6-1	$-0.93 \times 10^{-2}$	$0.29 \times 10^{-2}$
6-2	$-0.56 \times 10^{-2}$	$0.26 \times 10^{-2}$
6-3	$-0.51 \times 10^{-2}$	$0.26 \times 10^{-2}$
6-5	$-0.28 \times 10^{-2}$	$0.12 \times 10^{-2}$
2-1	$-0.58 \times 10^{-2}$	$0.12 \times 10^{-2}$
3-2	$0.34 \times 10^{-2}$	$0.12 \times 10^{-2}$
3-1	$0.28 \times 10^{-2}$	$0.14 \times 10^{-2}$

TABLE III. Regression coefficients of  $\dot{p}$  and  $\dot{g}$  on frequency derivatives  $f_{ij}$ .

Oscillator pair	Regression coefficient of $\dot{p}$	Regression coefficient of $\dot{g}$
5-1	-9.9	$-0.60 \times 10^{-4}$
5-2	-0.8	$-0.59 \times 10^{-4}$
5-3	5.5	$-0.43 \times 10^{-4}$
6-1	-31	$-0.80 \times 10^{-4}$
6-2	-21	$-0.79 \times 10^{-4}$
6-3	-16	$-0.62 \times 10^{-4}$
6-5	-21	$-0.22 \times 10^{-4}$
2-1	-10	$-0.01 \times 10^{-4}$
3-2	-6.4	$-0.16 \times 10^{-4}$
3-1	-16	$-0.17 \times 10^{-4}$

$$|\alpha_{ms} \text{ (diurnal)}| \leq 1.65 \times 10^{-2}. \quad (10)$$

#### IV. DISCUSSION OF RESULTS

##### A. Linear drift of frequency

We have seen that the maser frequencies increased relative to the SCSO's at rates of several parts in  $10^{14}$  per day. Frequency standards are often subject to long-term systematic drifts; in particular, it has recently been found that some hydrogen masers have slow upward drifts in frequency at a rate of up to 1 to 2 parts in  $10^{14}$  per day over time spans of many months.<sup>12</sup> This is believed to be due to settling of the ground joints of their resonant cavities. Over the year prior to this experiment, *M6*'s resonant cavity decreased in length at a rate corresponding to a change in output frequency of  $1.6 \times 10^{14}$  per day. Data on maser *M5*'s long-term cavity frequency drift are fragmentary; however, Table I shows that the 5-6 regression coefficient, and hence the drift rate between masers *M5* and *M6*, is small compared with those of other oscillator pairs, leading to the conclusion that *M5*'s frequency had a long-term behavior similar to that of *M6*. It appears, then, that the frequencies of both *M5* and *M6* drifted upward at rates of approximately  $(1 \text{ to } 2) \times 10^{-14}$  per day during the experiment due to resonant cavity deformation. A spontaneous frequency drift of  $1.6 \times 10^{-14}$  per day (equal to *M6*'s drift rate) due to the masers contributes to  $\alpha_{ms}$  approximately  $0.54 \times 10^{-2}$ , which is 40 percent of the value of  $\alpha_{ms}$  obtained in Eq. (9). Correcting  $\alpha_{ms}$  (linear) for this cavity-induced drift rate gives an upper bound for the 95-percent confidence interval of

$$|\alpha_{ms} \text{ (linear)}| \leq 1.5 \times 10^{-2}. \quad (11)$$

##### B. Diurnal frequency variations

As shown by the regression coefficients of Table III, changes in barometric pressure affect all the frequency differences, particularly those involving SCSO *S1* or maser *M6*. This is caused by the physical construction of the oscillators. The barometric sensitivities of the SCSO's may arise from the fact that they are suspended by wave guides from a plate covering their Dewar; changes in barometric pressure deflect the plate, which tilts the SCSO cavities, causing changes in cavity dimensions that alter the cavity resonance frequencies. Alternatively, the sensitivity may result from dispersion in the microwave electrons caused by changes in barometric pressure.

The masers' barometric sensitivities were measured following the experiment.<sup>13</sup> *M6*'s sensitivity was found to be approximately  $3 \times 10^{-13}$  per inch Hg, which is consistent with the results shown in Table III and is more than an order of magnitude greater than the sensitivities of other masers. When *M6* was subsequently disassembled, the anomalous barometric sensitivity was found to have been due to a mechanical interference within the maser, which was then corrected. In contrast, *M5* had no detectable barometric sensitivity; measurement uncertainty places an upper bound of approximately  $8 \times 10^{-15}$  per inch Hg on *M5*'s sensitivity.

The oscillators' barometric and gravitational sensitivities can affect the estimation of the diurnal solar effect in the following way. The local variation of  $g$ , and thus of the atmospheric tide, has a diurnal component in addition to the dominant semi-diurnal term.<sup>14</sup> Because the regression analysis does not yield a perfect fit of  $\dot{p}$  or  $\dot{g}$  to the frequency derivatives, some of the diurnal variation in the  $f_{ij}$  that is due to  $\dot{p}$  and  $\dot{g}$  correlates with  $\dot{u}$  and thus contributes to the  $a_{ij}$ . This is suggested by Table II: the regression coefficients  $a_{k6}$  ( $k=1,2,3$ ) for *M6*-SCSO pairs are approximately twice as large as the respective values of the  $a_{k5}$ .

##### C. Conclusion

The results of this experiment are consistent with the predictions of metric theories of gravitation, with the upper limit of  $\alpha_{ms}$  being given by  $\alpha_{ms}$  (diurnal) as

$$|\alpha_{ms}| \leq 1.7 \times 10^{-2}.$$

The limit given by  $\alpha_{ms}$  (linear), which is estimated from the frequency data uncorrected for long-term frequency drifts, is

$$|\alpha_{ms}| < 2.0 \times 10^{-2}.$$

After correction for cavity-induced maser frequency drift, this measure gives

$$|\alpha_{ms}(\text{linear})| \leq 1.5 \times 10^{-2}.$$

The latter two limits are more likely to be affected by unidentified systematic effects than is the former.

#### ACKNOWLEDGMENTS

This work was supported in part by the National Aeronautics and Space Administration (NSG8059). C.W. acknowledges support from the National Aeronautics and Space Administration (NSG-7204), the National Science Foundation (PHY79-20123), and the Alfred P. Sloan Foundation at Stanford University, and the National Science Foundation (PHY81-15800) at Washington University.

#### APPENDIX A: VARIATION OF THE FINE-STRUCTURE CONSTANT

One simple and heuristic model for violations of LPI is to assume that the locally measured electromagnetic fine-structure constant  $\alpha$  is a function of an external gravitational potential, while other constants (speed of light, particle masses, strong and weak interaction constants, etc.) are true constants. The frequency of the hyperfine transition in hydrogen and hence that of a hydrogen maser clock is given by

$$hf_{\text{HM}} = \Delta E_{\text{hf}} = \frac{8}{3}(e^2/2a_0)g_p(m_e/m_p)\alpha^2, \quad (\text{A1})$$

where  $g_p$  is the proton  $g$  factor,  $m_e/m_p$  is the electron-proton mass ratio, and  $a_0$  is the Bohr radius, given by

$$a_0 = \hbar^2/m_e e^2. \quad (\text{A2})$$

Equations (A1) and (A2) can be combined to yield

$$hf_{\text{HM}} = \frac{4}{3}(m_e g_p)(m_e/m_p)c^2\alpha^4 \propto c^2\alpha^4. \quad (\text{A3})$$

On the other hand, the frequency of an SCSO clock is determined by the size of the microwave cavity, which depends on the interatomic spacing in the material surrounding the cavity. This in turn depends on the Bohr radius. That is,

$$hf_{\text{SCSO}} = hc/\lambda \propto hc/a_0 \propto m_e c^2 \alpha \propto c^2 \alpha. \quad (\text{A4})$$

Thus the ratio of the frequencies of the two kinds of clocks is given by

$$f_{\text{HM}}/f_{\text{SCSO}} \propto \alpha^3(U). \quad (\text{A5})$$

#### APPENDIX B: ATOMIC CLOCKS IN THE $TH\epsilon\mu$ FORMALISM

It is useful to study the response of atomic clocks to gravitational fields within a more specific mathematical model that incorporates nonuniversal coupling explicitly. One such model is the  $TH\epsilon\mu$  formalism, developed by Lightman and Lee.<sup>15,16</sup> It deals with the motions and electromagnetic interactions of charged structureless test particles in an external, static, spherically symmetric gravitational field. Since the experiment described in this paper dealt with the behavior of atomic clocks in the solar field, this is an adequate model for the principal effects. The model assumes that the laws of electrodynamics can be derived from the classical action

$$\begin{aligned} I &\equiv I_0 + I_{\text{int}} + I_{\text{em}} \\ &\equiv - \sum_a m_{0a} \int (T - H v_a^2)^{1/2} dt \\ &\quad + \sum_a e_a \int A_\mu(x_a) v_a^\mu dt \\ &\quad + (8\pi)^{-1} \int (\epsilon E^2 - \mu^{-1} B^2) d^4x. \end{aligned} \quad (\text{B1})$$

We use units in which  $x$  and  $t$  have units of length. Here  $m_{0a}$ ,  $e_a$ , and  $x_a^\mu(t)$  are the rest mass, charge, and world line of particle  $a$ ,  $x^0 \equiv t$ ,  $v_a^\mu \equiv dx_a^\mu/dt$ ,

$$\vec{E} \equiv \vec{\nabla} A_0 - \vec{A}_0, \quad \vec{B} \equiv \vec{\nabla} \times \vec{A},$$

and where scalar products between three-vectors are taken with respect to the Cartesian metric  $\delta^{ij}$ . The functions  $T$ ,  $H$ ,  $\epsilon$ , and  $\mu$  are assumed to be arbitrary functions of an external gravitational potential  $U$ .

The metric postulates of Sec. I are satisfied if and only if the functions  $T$ ,  $H$ ,  $\epsilon$ , and  $\mu$  obey

$$\epsilon = \mu = (H/T)^{1/2} \quad (\text{B2})$$

for all  $U$ . If this is true, then all three pieces of the action  $I$  are universally coupled to the spacetime metric, whose components are given in this case by

$$g_{00} = -T, \quad g_{ij} = H\delta_{ij}, \quad g_{0j} = 0. \quad (\text{B3})$$

We shall first show how violations of LLI and LPI can occur in this model. (For violations of WEP, see Ref. 15.) We make a coordinate transformation to a frame that falls with the same acceleration  $\vec{g}$  as a neutral test particle, namely,

$$\vec{g} = -\frac{1}{2}H^{-1}T'\vec{\nabla}U, \quad (\text{B4})$$

where  $T' \equiv dT/dU$ . After appropriately rescaling the time and space coordinates, we put the action into the form



$$I = - \sum_a m_{0a} \int (1-v_a^2)^{1/2} dt + \sum_a e_a \int A_\mu v^\mu dt + (8\pi)^{-1} \epsilon T^{1/2} H^{-1/2} \int [E^2 - (T^{-1} H \epsilon^{-1} \mu^{-1}) B^2] d^4x, \quad (\text{B5})$$

where the functions  $T$ ,  $H$ ,  $\epsilon$ , and  $\mu$  are to be evaluated at the origin of the frame. We have ignored terms in the electromagnetic action of order  $\vec{g} \cdot \vec{x}$ , which lead to violations of WEP for electromagnetically interacting systems, and have ignored tidal terms  $O((x^\alpha)^2)$  throughout the action.<sup>5</sup>

The first two terms have the usual special-relativistic forms, but the third does not, unless Eq. (B2) is satisfied. If we now rescale the vector potential  $A_\mu$ , we can cast the action into the form

$$I = - \sum_a m_{0a} \int (1-v_a^2)^{1/2} dt + \sum_a e_a^* \int A_\mu v^\mu dt + (8\pi)^{-1} \int (E^2 - c^{*2} B^2) d^4x, \quad (\text{B6})$$

where  $e_a^*$  is a “rescaled charge,” given by

$$e_a^{*2} = e_a^2 \epsilon^{-1} (H/T)^{1/2}, \quad (\text{B7})$$

and  $c^*$  is a “speed of light” given by

$$c^{*2} = (H/T) (\epsilon \mu)^{-1}. \quad (\text{B8})$$

Notice that in this coordinate system, the limiting speed of neutral test particles, as determined from  $I_0$  in Eq. (B6), has been chosen to be unity. Although the  $I_0$  and  $I_{\text{int}}$  parts of the action are Lorentz invariant, the electromagnetic action is not, unless  $c^* \equiv 1$  for all  $U$ . In this way local Lorentz invariance may be violated. Even if  $c^* \equiv 1$ , the renormalized charge  $e_a^*$  may depend upon location unless

$$\epsilon^{-1} (H/T)^{1/2} = \text{const}.$$

In this way, local position invariance may be violated. If  $c^* \equiv 1$ , we see that the theory described by Eq. (B6) is equivalent to the varying-fine-structure-constant model discussed in Appendix A. In any case, Eqs. (B7) and (B8) show that the “rescaled” fine-structure constant  $\alpha^*$  is related to  $T$ ,  $H$ ,  $\epsilon$ , and  $\mu$  by

$$\alpha^* = \alpha (\mu/\epsilon)^{1/2}. \quad (\text{B9})$$

Within the  $TH\epsilon\mu$  formalism, the behavior of atomic clocks may be determined in detail by quantizing the dynamics embodied in Eq. (B1).<sup>17</sup> For our purpose it suffices to consider a hydrogen atom consisting of a proton of mass  $m_p$ , charge  $e$ , and magnetic moment  $\vec{M}_p$ , and an electron of mass  $m_e$  and charge  $-e$ . The atom is at rest in the  $TH\epsilon\mu$  coordi-

nate system. In the semirelativistic limit, the quantum-mechanical Hamiltonian obtained from Eq. (B1) has the form

$$H = H_r + H_s + H_f + H_{\text{hf}} + O((p^2/m_e)^3), \quad (\text{B10})$$

where the four terms in  $H$  are the usual rest mass, Schrödinger, fine-structure, and hyperfine-structure contributions, given by

$$H_r = T_0^{1/2} m_e, \quad (\text{B11})$$

$$H_s = T_0^{1/2} H_0^{-1} \frac{p^2}{2m_e} - \epsilon_0^{-1} \frac{e^2}{r}, \quad (\text{B12})$$

$$H_f = -T_0^{1/2} H_0^{-2} \frac{p^4}{8m_e^2} - H_0^{-1} \epsilon_0^{-1} (e^2 \hbar / 4m_e^2 r^3) \vec{\sigma} \cdot \vec{L}, \quad (\text{B13})$$

$$H_{\text{hf}} = T_0^{1/2} H_0^{-1} (e \hbar / 2m_e) \vec{\sigma} \cdot \vec{B}, \quad (\text{B14})$$

where  $\vec{L} = \vec{x} \times \vec{p}$  is the angular momentum of the electron,  $\vec{\sigma}$  are Pauli spin matrices, and  $\vec{B}$  is the magnetic field of the proton, given by

$$\vec{B} = -\frac{1}{2} \mu_0 \{ [\vec{M}_p - 3\vec{n}(\vec{n} \cdot \vec{M}_p)] r^{-3} - (8\pi/3) \vec{M}_p \delta^3(\vec{x}) \} \quad (\text{B15})$$

where  $\vec{n} = \vec{x}/r$ . We have ignored the Darwin term in  $H$ . By analogy with the expression for the magnetic moment of the electron in the hyperfine term Eq. (B14), we identify the magnetic moment of the proton as

$$\vec{M}_p = T_0^{1/2} H_0^{-1} (g_p e \hbar / 2m_p) \vec{\sigma}_p, \quad (\text{B16})$$

where  $g_p$  is the gyromagnetic ratio of the proton, assumed to be independent of position.

It is then straightforward to show that the principal (Schrödinger) energy levels of hydrogen are given by

$$E_p = (-m_e e^4 / 2 \hbar^2 n^2) (T_0^{-1/2} H_0 \epsilon_0^{-2}), \quad (\text{B17})$$

where  $n$  is an integer. The Bohr radius is given by

$$a_0 = (\hbar^2 / m_e e^2) (T_0^{1/2} H_0^{-1} \epsilon_0). \quad (\text{B18})$$

Similarly, from  $H_{\text{hf}}$ , the energy of the lowest hyperfine transition of hydrogen is given by

$$\Delta E_{\text{hf}} = \frac{4}{3} m_e (e^4 / \hbar^2)^2 g_p (m_e / m_p) \times (T_0^{-1/2} H_0 \epsilon_0^{-3} \mu_0). \quad (\text{B19})$$

From the canonical Hamiltonian for the electromagnetic field obtained from Eq. (B1) we find that the energy of an electromagnetic mode in a microwave cavity is given by

$$E_c = (N + \frac{1}{2})\hbar\omega, \quad (\text{B20})$$

where  $N$  is the number of quanta and  $\omega$  is the resonant frequency of the cavity, related to the wave number  $k$  by the dispersion relation

$$|\vec{k}|^2 - \epsilon_0\mu_0\omega^2 = 0. \quad (\text{B21})$$

For a stationary mode,  $|\vec{k}| \propto L^{-1}$ , where  $L$  is the length of the cavity, itself proportional to the Bohr radius  $a_0$ . Thus

$$|\vec{k}| \propto T^{-1/2}H_0\epsilon_0^{-1},$$

and

$$E_c = E^{(0)}(T_0^{-1/2}H_0\epsilon_0^{-3/2}\mu_0^{-1/2}), \quad (\text{B22})$$

where  $E^{(0)}$  depends only on atomic constants and integers. To determine the predicted position dependence of the ratio of hydrogen maser and SCSO frequencies, we take the ratio of Eqs. (B19) and (B22) to obtain

$$f_M/f_S = (f_M/f_S)_0(\mu_0/\epsilon_0)^{3/2}. \quad (\text{B23})$$

Thus, with this formalism the null gravitational red-shift limits the spatial variation of  $(\mu_0/\epsilon_0)^{3/2}$ . If EEP is satisfied,  $\mu_0/\epsilon_0 \equiv 1$ .

\*Present address.

<sup>1</sup>A. Einstein, *Jahrb. Radioact. Elekt.* **4**, 411 (1907).

<sup>2</sup>For a review, see C. M. Will in *General Relativity: An Einstein Centenary Survey*, edited by S. W. Hawking and W. Israel (Cambridge University, Cambridge, England, 1979).

<sup>3</sup>R. F. C. Vessot and M. W. Levine, *Phys. Rev. Lett.* **45**, 2081 (1980).

<sup>4</sup>K. S. Thorne, D. L. Lee, and A. P. Lightman, *Phys. Rev. D* **7**, 3563 (1973).

<sup>5</sup>C. M. Will, *Theory and Experiment In Gravitational Physics* (Cambridge University, Cambridge, England, 1981).

<sup>6</sup>M. P. Haugan, *Ann. Phys. (N.Y.)* **118**, 156 (1979).

<sup>7</sup>C. W. Misner, K. S. Thorne, and J. A. Wheeler, *Gravitation* (Freeman, San Francisco, 1973), Sec. 38.5.

<sup>8</sup>R. H. Dicke, in *Relativity, Groups, and Topology*, edited by B. DeWitt and C. DeWitt (Gordon and Breach, New York, 1964); J. D. Bekenstein, *Phys. Rev. D* **25**, 1527 (1982).

<sup>9</sup>J. P. Turneure and S. R. Stein, in *Atomic Masses and Fundamental Constants*, edited by J. H. Sanders and A. H. Wapstra (Plenum, New York, 1976), Vol. 5, p. 636.

<sup>10</sup>D. Kleppner, H. C. Berg, S. B. Crampton, N. F. Ramsey, R. F. C. Vessot, H. E. Peters, and J. Vanier, *Phys. Rev.* **138**, A972 (1965).

<sup>11</sup>S. R. Stein and J. P. Turneure, *Proc. IEEE* **63**, 1249 (1975); S. R. Stein and J. P. Turneure, *Electron. Lett.* **8**, 321 (1972).

<sup>12</sup>P. Kuhnle, Jet Propulsion Laboratory, Pasadena, California, private communication.

<sup>13</sup>P. Kuhnle and A. Kirk, Jet Propulsion Laboratory, Pasadena, California, private communication.

<sup>14</sup>Paul Melchior, *The Tides of the Planet Earth* (Pergamon, Oxford, 1978).

<sup>15</sup>A. P. Lightman and D. L. Lee, *Phys. Rev. D* **8**, 364 (1973).

<sup>16</sup>For other formalisms see Ref. 6, and W.-T. Ni, *Phys. Rev. Lett.* **38**, 301 (1977).

<sup>17</sup>C. M. Will, *Phys. Rev. D* **10**, 2330 (1974).